IEEE Access
Multidisciplinary | Rapid Review | Open Access Journal

Received November 8, 2019, accepted February 1, 2020, date of publication February 24, 2020, date of current version March 4, 2020.

*Digital Object Identifier 10.1109/ACCESS.2020.2975879*

# Shared LTE Network Performance on Smart Grid and Typical Traffic Schemes

**JUHO MARKKULA, (Student Member, IEEE), AND JUSSI HAAPOLA, (Member, IEEE)**
Centre for Wireless Communications (CWC), University of Oulu, 90014 Oulu, Finland

Corresponding author: Juho Markkula (juho.markkula@oulu.fi)

This work was supported by the Academy of Finland 6Genesis Flagship under Grant 318927.

**ABSTRACT** This paper investigates the possibility of delivering distinct smart grid (SG) demand response (DR) applications in a highly loaded LTE network. In a shared LTE network, the proportion of SG DR traffic is relatively low when compared to typical traffics such as voice over IP, Skype video call, FTP, Youtube video stream, and HTTP. The quality of service (QoS) requirements for the SG DR traffics have to be fulfilled by maintaining the network delays and the packet delivery ratios within certain limits, while not causing significant hindrance to the typical traffics. The Riverbed Modeler network simulations are performed using detailed physical layer propagation models, detailed LTE functionality, and a suburban topology. In the simulation scenarios, three distinct DR applications generate varying amounts of SG DR traffic to the LTE network while the LTE capacity is exceeded by the typical traffics. The results illustrate that satisfactory performance for the SG DR traffics can be maintained due to the constant traffic characteristics and relatively low traffic amount that facilitates the scheduling of channel resources. Typically, the more a DR application generates traffic the higher hindrance it causes for the typical traffics other than the voice over IP that applies the QoS class of highest priority.

**INDEX TERMS** Demand response, Internet of Things, LTE, smart grid communications.

## I. INTRODUCTION

Advanced metering infrastructure (AMI) is a combination of smart meters, a communication network, and utility systems [1]. The communication network enables two-way communications between the smart meters and the utility system that contains a metering data management system (MDMS). A remote terminal unit (RTU) is a communication interface that is connected to a smart meter and transmits information, collected by the smart meter, to a MDMS that processes it and delivers feedback. The main focus of AMI is to provide real-time information and control of household electricity consumption and local energy production for demand response (DR) applications, but also conventional automatic meter reading (AMR) functionalities such as automatic consumption metering, diagnostic, and status data collection are included for billing and analysis purposes. Wireless communications are an essential part of the communication path due to the low installation costs and reduced cabling, and there are various options for the applied wireless communication technology such as long term evolution (LTE), narrowband IoT (NB-IoT), LoRaWAN, IEEE 802.15.4, and IEEE 802.11. Powerline communications come also at zero cabling costs, but cannot provide such a high bit-rates, reliability, and wide networks as wireless communications [2].

Lately, there has been a rapid growth in distributed energy resources (DER) such as distributed generation and energy storages connected to the distribution network, and micro-generation concurrently with flexible loads at the premises of the end users [3], [4]. Estimates disclose that renewable energy sources based on solar, wind, geothermal, and tides can meet a large portion of the energy demand [5]–[7]. These resources are not actively utilized at the distribution system by distribution network operators, retailors, or energy service providers, as there are no active markets in place to boost DERs at the edge of the grid. The demand side flexibility provided by the DR applications is the main enabler to allow the optimum operation of DER by making possible novel business models introduced in [8] were surplus energy can be traded between the consumers and the prosumers inside and between the micro grids or traded to the wholesale markets, and the prices can be selected to balance the offer and demand within each micro grid. To reduce power consumption peaks due to DR programs, a smart meter could provide the current

The associate editor coordinating the review of this manuscript and approving it for publication was Zhong Fan.

energy consumption value and a metering data management system could specify the electricity price due to the total consumption of multiple smart meters [9], [10], a system operator could turn on/off each user's device according to a direct load control program that follows the grid state and the defined load shaping policy [11], or renewable energies may be utilized during the highest grid load.

### A. RELATED WORKS

In [12], the authors investigated if a public LTE network is suitable for smart grid (SG) automatic meter usage without causing significant hindrance to typical public LTE traffic. Based on the simulation results, regular SG traffic has very little effect on the LTE base station, called evolved universal terrestrial radio access node B (eNB), or the network load. When considering critical emergency events, such as blackout last gasp messaging, with hundreds of simultaneous packet generations, the network resource allocation capacity was exceeded. Two proposed solutions for mitigating network overloading were effective. The first solution was adding the artificial, [0, 1) s random delay for packet transmissions. The second solution was applying a hybrid sensor-LTE network where RTUs first transmit data to their CLH that contains both an IEEE 802.15.4 and an LTE communication interface. In [13], the authors simulated SG DR scenarios in an LTE and a hybrid sensor-LTE network. There were some differences in performances between these two networks. Applying the hybrid sensor-LTE network appeared to have a lower impact on the typical public LTE traffic because the antennas of CLHs were located outside on the rooftop height, not inside the houses as RTUs in the LTE network. In [14], the authors presented a solution to overcome issues relating to lack of LTE base station connectivity for user equipment (UE) considered as RTUs. The solution is an ad hoc mode for the LTE-Advanced UE. The ad hoc mode is applied to reach a relay node that is the nearest UE with base station connection. DR traffic is delivered between clusters of UE and a relay node using multi-hop communications. Previously, the authors researched the influence of a highly loaded public LTE network for the SG DR traffic delivery [15]. Various amounts of typical traffics were generated to exceed the network capacity, and the effects of quality of service (QoS) class selection for SG DR traffic components were researched. The results illustrated that the SG DR traffic, with constant traffic characteristics, can be delivered also in a highly loaded network when the capacity is exceeded, maintaining satisfactory DR communications performance. It was not reasonable to lower the QoS of the RTUs that transmitted in uplink (UL) direction, because the SG DR traffic (UL) delay increased and the packet delivery ratio (PDR) decreased remarkably already with the lowest typical traffic volume. The SG server transmits in downlink (DL) direction and the QoS could be lowered without significant hindrance for the SG DR control traffic (DL) performance, because the DL channel capacity is remarkably higher than the UL channel capacity. However, lowering the QoS of SG DR traffic did not significantly improve the typical LTE traffic performance.

In [16], a feasibility assessment of seven distinct communications technology solutions was performed, using 28 key performance indicators, to estimate their superiority for SG applications such as grid control, AMR, and DR. When concerning the technologies of our research, the LTE with an ad hoc mode obtained the lowest total feasibility points (25.96%) for the DR communications. The second was the LTE network with the points of 28.28%. The best feasibility points, 34.07%, were obtained by the hybrid sensor (IEEE 802.15.4)-LTE network. All these three technologies equally fulfilled the reliability and latency requirements. There were small differences in the feasibility points of the metrics: number of supported users, robustness, and security. The LTE network obtained the best points in all these three metrics having 14.29% as the sum of these three metrics. The hybrid sensor-LTE network got the sum of 12.65%, and equal points as the LTE network in robustness. The LTE with an ad hoc mode obtained the same points as the LTE network in security having 11.96% as the sum. The hybrid sensor-LTE network obtained 7.4 units better results in cost metric that contains the expenses of all communication devices, coordinator devices, personnel for training and maintenance, development and subscription. It is obvious that the decreased number of LTE UE due to the clustered sensor-LTE network reduces the expenses of the subscriptions and communication devices. However, an IEEE 802.15.4 network is operated on unlicensed frequency bands where the other devices may cause interference when transmitting concurrently on the same frequency. Considering this aspect may lower the total feasibility of the hybrid solution, perhaps below the two other solutions.

In [17], an LTE FDD and TDD network simulation study using Opnet modeler is performed in a typical SG scenario to research the effect of packet size for UL transmissions. The results show that FDD outperforms TDD in terms of UL delay, and the TDD network benefit is that the split of UL/DL resources can be easily adapted to match the UL bias of the offered traffic. LTE UL resource scheduling policy seems to cause a step increase in delay and channel utilization with the application packets larger than 40 bytes. The UL scheduling strategy to facilitate the coexistence of smart meters and typical UE in the LTE network is proposed in [18]. The scheduler considers service differentiation, delay constraints, and channel conditions, and it utilizes relays to decrease the number of direct smart meter connections to the eNB. In [19], the LTE network performance is increased by applying a combination of contention and non-contention based random access procedures for smart meters to establish connections and by delivering SG traffic via tracking area update control signaling to conserve resources at the eNB for typical data transmissions. Limitations of signaling constraints in the random access and control channels are explored with LTE access reservation protocol simulations using machine-to-machine (M2M) traffic [20]. A more efficient procedure in case of M2M connection establishment should be considered

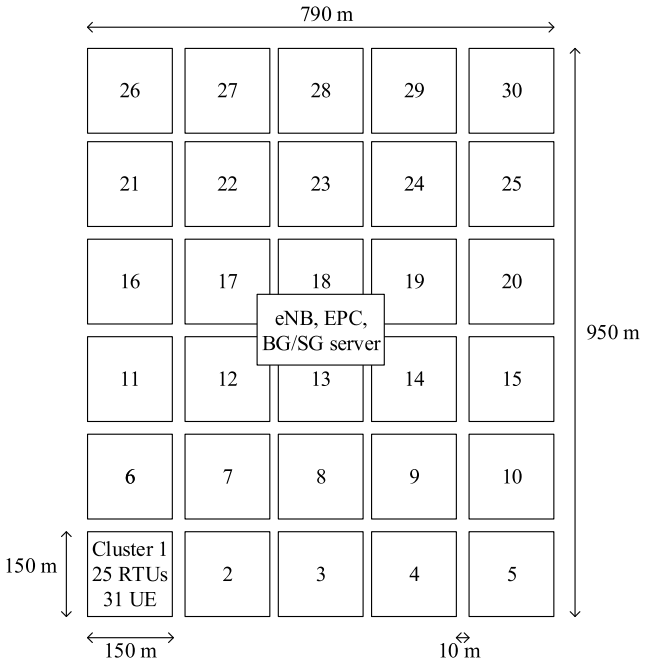


**FIGURE 1.** Evaluated, generalized suburban scenario topology with 750 RTUs and 930 UE. In each cluster the RTUs and UE are randomly positioned.

by taking into account the features of the actual channels. In [21], a shared LTE network is consider by reserving distinct number of resource blocks for SG traffic that is generated by phasor measurements units, power measurements and control devices, and smart meters. The network performance such as latency and reliability are evaluated and some improvements for security framework and random access mechanism are presented.

### B. CONTRIBUTION OF THIS PAPER

This paper's contribution is to provide new results and discussion to complete the research of the three previous conference papers and one journal paper [12]–[15]. As also in the previous articles, the Riverbed Modeler network simulator is used with detailed physical layer propagation models, detailed LTE functionality, a suburban topology, and multiple overlapping applications for SG and public LTE network communications. The suburban topology (Fig. 1) is formed based on a realistic suburban environment where 930 UE and 750 RTUs are using the same operator and the base station.

In this paper, the influence of a highly loaded LTE network for the SG DR traffic delivery is researched to achieve a holistic picture of SG operations. Furthermore, the simulation results are analyzed accurately to discover possible simulator and computational restrictions that may have effected to the results. In the simulation scenarios, three distinct DR applications generated various amounts of SG DR traffic to the LTE network while the capacity was exceeded with typical traffics such as voice over IP, Skype video call, FTP, Youtube video stream, and HTTP. Network simulations were performed to research the possibility of delivering SG DR traffics while maintaining the QoS requirements for the network delay and the PDR, and not causing significant hindrance to the typical traffics. The proportion of SG DR traffic is relatively low when compared to the typical LTE traffic. In addition, SG DR traffic is mainly transmitted in UL direction contrary to the typical traffic that is mostly generated in DL direction. SG DR traffic may cause hindrance for some typical traffic applications, because the UL channel capacity is remarkably lower than the DL channel capacity. In addition, smart meters may be placed in locations, such as basements, where the pathloss weakens the signal and causes additional traffic by the lower modulation, additional error correction code, and retransmissions. SG traffic is typically generated with constant intervals that may enable its successful delivery also in a highly loaded network.

The contribution of the first article [12] was to investigate the feasibility of a public LTE network in supporting worst case SG communications and still providing acceptable performance for regular LTE traffic. In addition, an IEEE 802.15.4-based, hybrid sensor-LTE network was simulated to observe if one or the other approach shows a clearly better performance in terms of satisfying QoS criteria of emergency and AMR traffic. The contribution of the second article [13] was to investigate the range of DR scenarios that can be satisfied by either LTE or/and hybrid sensor-LTE communications and with what fidelity. In this paper, the results of [13] are further discussed by utilizing the information obtained from the current results. The journal paper [14], presented an ad hoc mode for an LTE-Advanced UE to maintain DR communication when there is lack of base station connectivity. The contribution of the third article [15] was to research the influence of a highly loaded LTE network for the SG DR traffic delivery. Various amounts of typical traffics were generated to exceed the public LTE network capacity, and the effects of QoS class selection for SG DR traffic components were researched. In this paper, the simulations of [15] were refined when the different DR applications were applied instead of observing the effects of QoS class selections. In addition, discontinuous reception (DRX) capability was disabled, because it seemed to cause some inaccuracy for the network delay results due to the modeling of multiple RTUs or UE by a single node.

The rest of the paper is organized as follows. Section II proposes the system description introducing the simulation model, the channel model, and the applied key parameters. In Section III the simulation scenarios are presented, and the results are shown in Section IV. Section V discusses the current and the previous results of the topic with critical aspect, and Section VI concludes the paper with further holistic observations.

## II. SYSTEM DESCRIPTION

### A. SIMULATION MODEL

The Wireless Suite and LTE simulation toolboxes of Riverbed Modeler were utilized in the simulations [22]. Fig. 2 presents

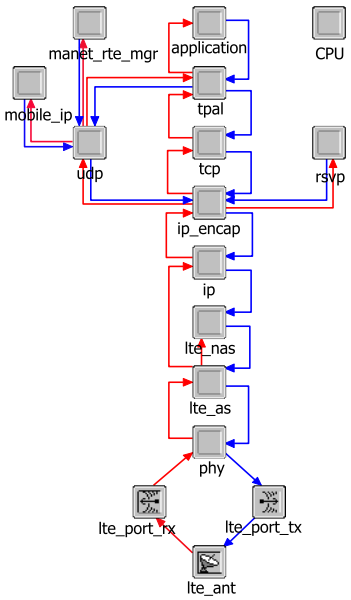


**FIGURE 2.** The LTE UE node model of the Riverbed Modeler network simulator.

the LTE UE node model that includes multiple blocks each containing a communication protocol. A block is implemented as one or multiple process models. A process model contains C code also including Riverbed Modeler specific functions. For example, the process model of the "lte_as" block contains radio resource control (RRC), radio link control (RLC), and media access control (MAC) layer functionalities of a UE. "lte_as" block is connected through the physical layer "phy" block to the receiver "lte_port_rx" and the transmitter "lte_port_tx" blocks. These two blocks communicate with the antenna "lte_ant" block. The simulations are performed in packet level. Occurring events produce interrupts to distinct process models to perform actions, e.g. a packet is generated in the process model inside the "application" block. A packet traverses through the blocks between the application and the antenna while some headers are added or removed on a path.

Fig. 3 shows the LTE eNB node model that has a wireless connection with the LTE UE through the antenna "lte_ant" block. One of the wired ethernet connections with the receiver "eth_rx" and the transmitter "eth_tx" blocks is connected to the evolved packet core (EPC). "lte_as" block of the base station contains RRC, RLC, and MAC layers. For example, in these layers: connections and radio bearers for UE are established and released, hybrid automatic repeat request (HARQ) is applied for retransmissions and data combining, and channel resources for the UL and DL transmissions are scheduled.

### B. DESCRIPTION OF THE CHANNEL MODEL

Communications of the simulation scenario take place in a suburban environment. Outdoor and building entry losses were considered for the communications channels between

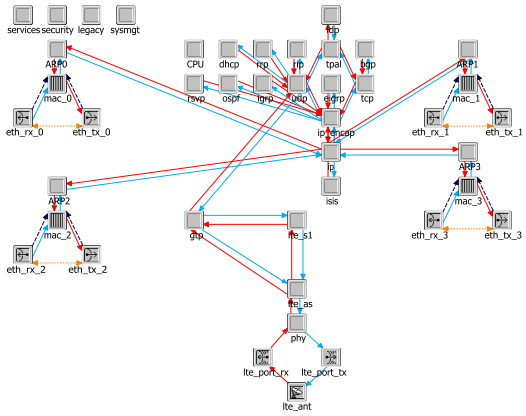


**FIGURE 3.** The LTE eNB node model of the Riverbed Modeler network simulator.

the UE/RTUs and the eNB [23]. LTE exploits orthogonal frequency division multiplexing (OFDM). Frequency variable channel appears flat over the narrow band of an OFDM subcarrier eliminating the need of complex equalization [24]. Solely narrowband fading occurs, which justifies narrowband radio channel modeling to be applied in evaluation of the LTE channel. Outdoor pathloss is the most significant source of attenuation for the signal, and we apply a macrocell pathloss model for suburban environments that is based on the empirical, modified COST231 Hata urban propagation model [25]. The path-loss ($\mathrm{PL}_H$) is

$$\begin{aligned}\mathrm{PL}_H[dB] = &\left(44.9 - 6.55\log_{10}(h_{bs})\right)\log_{10}\left(\frac{d}{1000}\right)\\ &+ 45.5 + (35.46 - 1.1h_{ms})\log_{10}(f_c)\\ &- 13.82\log_{10}(h_{bs}) + 0.7h_{ms} + C, \qquad (1)\end{aligned}$$

where $h_{bs}$ is the eNB antenna height in meters, $h_{ms}$ is the UE/RTU antenna height in meters, $f_c$ is the carrier frequency in MHz, $d$ is the distance between an eNB and an UE/RTU in meters, and $C = 0$ dB is a constant factor for suburban macrocell environment. According to the device heights and the topology presented in the Fig. 1, $d$ varies between 29 and 618 m for UE and RTUs in the LTE network.

In addition to the above-mentioned outdoor pathloss model, we consider building entry loss that is caused by the signal penetration trough the building walls [26]. Each wall attenuates the signal by approximately 6 dB causing slow fading [27]. The number of the walls is randomly selected between 0 and 2 causing 0, 6, or 12 dB attenuation for transmitted or received signals for each of the RTUs/UE. This is done to reflect the random positioning of the smart meters (on the side of a building) and the UE (inside or outside a building) with respect to the eNB. Modeling fast fading is not necessary due to static devices, i.e., the time variations of the radio channel properties are minimal or very slow [28].

### C. PARAMETERS

Key parameters for the LTE network (Table 1) are selected by taking into account the simulation topology and the

**TABLE 1.** Key parameters for the simulation scenarios.

| LTE parameter | RTU/UE | eNB |
|---|---|---|
| Bandwidth | 10 MHz (UL) | 10 MHz (DL) |
| Base frequency | 1800 MHz | 1990 MHz |
| Transmission power | 24 dBm | 43 dBm |
| Tx antenna gain | -0.2 dBi | 16.5 dBi |
| Receiver sensitivity | -106.5 dBm | -120.7 dBm |
| Antenna height | 1.5 m | 30 m [SISO] |
| Cyclic prefix type | 7 symbols per slot | |
| Scheduling mode | Link adaption and channel dependent scheduling | |
| HARQ retransmissions | Max. 3 | |
| RLC retransmissions | Max. 4 (RTU), 0 (UE) | |
| PDCP compression ratio | UDP/IP: random [0.5714-0.7143], TCP/IP: random [0.1-0.4], RTP/UDP/IP: random [0.1-0.15] | |
| DRX | DRX capability: disabled<br>Short DRX cycle timer: 20 ms<br>Long DRX cycle multiplication factor: 4<br>On duration timer: 10 ms<br>Inactivity timer: 40 ms<br>Wake-up Policy for uplink data: Wake up immediately<br>Retransmission timer: 4 ms | |

technical specifications [29], [30]. The single input single output (SISO) antenna configuration is applied. The link adaptation and channel dependent scheduling mode signifies that also RTUs/UE will take measurements on various sub-bands and calculate separate modulation and coding scheme (MCS) indexes for each sub-band [24]. The eNB will try to match the RTUs/UE to their preferred sub-bands, perform link adaptation, and create a wideband MCS index. An RTU/UE transmits a scheduling request in physical UL control channel (PUCCH) to the eNB when traffic arrives to one of its empty buffers [24]. An RTU/UE is allowed to use PUCCH every 5 subframes. The eNB replies with a scheduling grant admitting the RTU/UE to transmit (in PUSCH) four subframes after receiving the scheduling grant. The scheduling request and grant are delivered without transmission errors in the simulations. HARQ retransmission [24] are enabled for all the SG and typical traffics, but RLC retransmissions are solely applied for the SG traffic to improve the reliability. Internet protocol (IP) related headers (IP, UDP, TCP, and RTP) are compressed using the packet data convergence protocol (PDCP) [24]. The DRX [24] capability is disabled. Thus, the receiver is constantly on and not turned off to conserve the battery. The DRX capability was applied in the previous conference paper [15], and the DRX functionality is explained in the Section V.

## III. SCENARIO SETUP

### A. INTRODUCTION TO THE SCENARIO

Fig. 1 presents the simulation topology that is a generalization of a suburban environment, where the gaps between clusters represent discontinuations in house clusters, like roads, streams, parks, etc. The clusters themselves represent municipal planning of groups of houses with less order in positioning (random placement of RTUs/UE). The terrain of the suburban region is quite flat and it is divided into 30 clusters, each containing 25 and, in total 750, houses/apartments with DR units, each equipped with RTUs. Every RTU is wirelessly connected with the eNB, and the SG server considered as an utility system has a wired connection with the EPC and the eNB. Smart grid traffic is delivered between the RTUs and the SG server.

It is assumed that a house hosts an average family size of 3.7 persons, each with a single UE, and there are three network operators with equal shares of users. Thus, there are in total 930 UE in the area using the same operator as the RTUs, and each cluster contains 31 UE producing typical traffic in the LTE network as background (BG) traffic. Solely one operator is applied for all SG traffic to model a situation with higher load than if the SG traffic would be shared among three operators. A public LTE network of an operator is used for SG traffic without any modifications to the typical LTE network configuration. The RTUs and the UE are randomly (with uniform distribution) positioned inside every cluster at the start of the each simulation run. The purpose of the random placement is to let the DR units to be placed in various locations, not dictated by municipal planning as is usual in real environments. Twenty different setups (each 20 min) that also affect the traffic distributions are averaged per each scenario. In total, from 85 to 95 million data packets were generated in every scenario.

### B. SIMULATION SCENARIOS

All the scenarios were simulated in an LTE network with exactly the same LTE parameters (Table 1). Traffic parameters of distinct traffic components are presented in Table 2. Smart grid traffic is generated according to the three different SG cases (1, 2, 3) in which each of the 750 RTUs transmits the energy usage updates to the SG server that transmits adjustments for every RTU. The SG case 1 scenario presents simulations in which accumulated energy usage updates (four second interval) are transmitted by RTUs and the SG server provides spot pricing adjustments to the RTUs at five-minute intervals in order to balance out the network load. The SG case 2 scenario presents simulations in which the frequency of instantaneous energy usage updates (one second interval) in the SG case 2 enables a control of local energy production when the SG server performs adjustments every 30 seconds. For example, local renewable energy production, such as solar power, could be utilized as extra energy during the energy consumption peaks. In the SG case 3, a high-intensity load balancing is performed when also the reporting of SG server is increased to provide adjustments once a second.

Four BG traffic amounts are considered in all the SG cases. All the 930 UE communicate voice over IP traffic. The other BG traffics (Skype video call, FTP, Youtube video stream, and HTTP) are generated by 33, 50, 67, and 100% of the UE. BG traffic is produced by the UE in UL and by the BG server in DL, and it was modeled as typical busy hour traffic that contains realistically modeled applications. UL traffic was

**TABLE 2.** Traffic parameters of distinct traffic components for 750 RTUs and 33, 50, 67, and 100% of the 930 UE.

| **Smart grid traffic per RTU (UL) and Server (DL)** | | **Start time** | | **Generation interval** | **Payload data** |
|---|---|---|---|---|---|
| SG DR (UL): | SG case 1 | random [300-304] s | | 4 s | 800 b |
| | SG case 2, 3 | random [300-301] s | | 1 s | |
| SG DR control (DL): | SG case 1 | random [300-600] s per each RTU | | 5 min | |
| | SG case 2 | random [300-330] s per each RTU | | 30 s | |
| | SG case 3 | random [300-301] s per each RTU | | 1 s | |
| **BG traffic per UE in an hour** | | **Start time** | **Session length/size** | | **Direction (UL/DL)** |
| Voice over IP (AMR 12.2k) | | 5 min | 2.5 min (silence length: 2 s, talksprut length: random [30-40] s) | | 50/50% |
| Skype video call (640p/30fps) | | | 30 s | | |
| FTP | | | 2 files (23.2 Mb/file) | | |
| Youtube video stream (720p/24fps) | | | 1 min | | 0/100% |
| HTTP | | | 2 pages (24 Mb/page) | | |
| Total BG application traffic | | | 250.9 Mb | | 21/79% |
| **LTE traffic component** | | **QoS class identifier, ARP** | | **GBR** | **Transport layer protocol** |
| Smart grid traffic | | 9 (non-GBR), 9 | | - | UDP |
| Voice over IP | | 1 (GBR), 2 [PDB: 100 ms] | | 96 kb/s | RTP/UDP |
| Skype video call | | 2 (GBR), 4 [PDB: 150 ms] | | 1.5 Mb/s | UDP |
| FTP, Youtube video stream, HTTP | | 9 (non-GBR), 9 | | - | TCP, UDP, TCP |

about 21% of the total traffic being at the realistic maximum level [32]. The amount of the BG traffic was relatively high because Skype video call and Youtube video stream were selected to have a high quality, and FTP files, e.g. photos, were also uploaded by the UE. Thus, the purpose was to reach the capacity limits of the network with BG traffic, and to observe the influence of a highly loaded LTE network for the various SG DR applications.

SG traffic applies the QoS class with the lowest priority. QoS class identifier (QCI) number 9 signifies that there is no guaranteed bit-rate (non-GBR) value for the transmitted data, unlike QCIs 1 and 2 have guaranteed bit-rate (GBR) values and lower allocation retention priority (ARP) values admitting a higher priority for evolved packet system (EPS) bearer creation and preservation [31]. The scheduler used in the simulator first allocates bandwidth for the QCIs 1 and 2 with objective to maintain the packet delay budget (PDB) by using the GBR values that are selected to be the same for the UL and DL. The priority indexes for the QCIs 1, 2, and 9 are 0, 2, and 3, respectively, in which the smaller number corresponds to a higher priority. The equal capacity algorithm allows to share the remaining channel capacity equally with traffic queues using the same priority index. The channel bandwidth is served first for the traffic queues with the higher priority. The traffic of QoS classes (QCI: 1 or 2) that cannot be delivered using GBR, e.g. GBR is not sufficiently high for all the generated traffic, the equal capacity algorithm is used to allocate bandwidth. Lastly, the scheduler allocates bandwidth for the QoS class with the lowest priority (QCI 9) using an equal capacity algorithm.

## IV. RESULTS

### A. LOADS OF TRAFFIC COMPONENTS

The Fig. 4 presents the average application loads for the SG and BG traffics as a function of traffic volume. Overheads of LTE and IP related headers are not included in the loads.

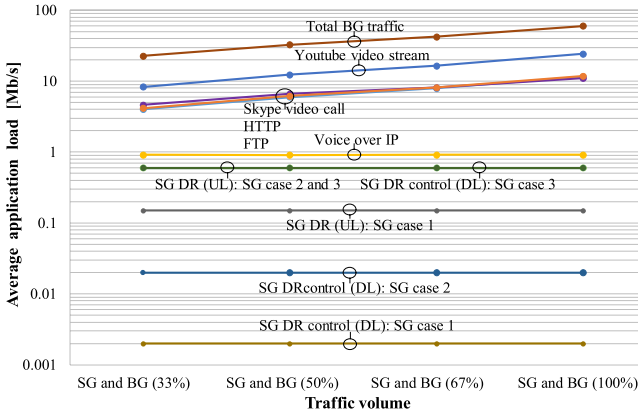


**FIGURE 4.** Average application loads of SG and BG traffic components.

The SG traffics for the SG cases 1, 2, and 3 are approximately 0.15, 0.6, and 0.6 Mb/s in UL, and 0.002, 0.02, and 0.6 Mb/s in DL direction, respectively. The volume of the BG traffic changes due to the percentage of the UE communicating also Skype video call, FTP, Youtube video stream, and HTTP traffics. In addition, all the UE participate in voice over IP communication with approximately the same traffic amount. Volume of the BG traffic components was clearly above the SG traffic. With the traffic volume, SG and BG (33%), the lowest amount of the total BG traffic (22.17 Mb/s) was generated when 33% of the UE were generating also other BG traffic components than voice over IP. The traffic volume, SG and BG (100%), corresponds to the highest amount of the total BG traffic (60.45 Mb/s) that was generated when each UE communicated using all the BG traffic applications.

### B. THROUGHPUTS OF TOTAL, DL, AND UL TRAFFICS

The Fig. 5 presents the average application load (solid lines) and throughput (square dotted lines) values of the total, DL, and UL traffics as a function of traffic volume in the SG cases 1, 2, and 3. It can be seen that with the traffic volume,

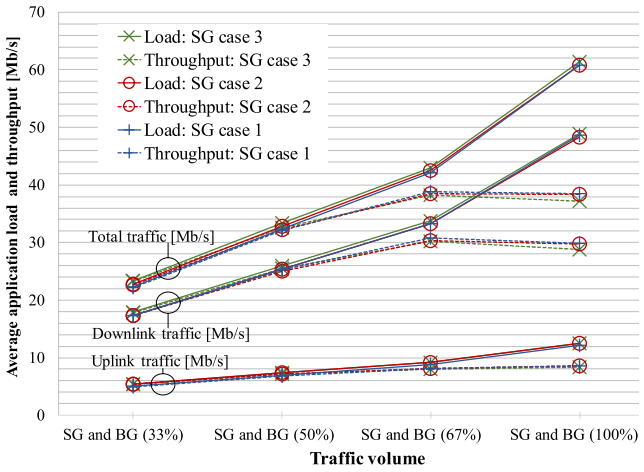


**FIGURE 5.** Average application loads and throughputs of total, DL, and UL traffics in megabits per second.

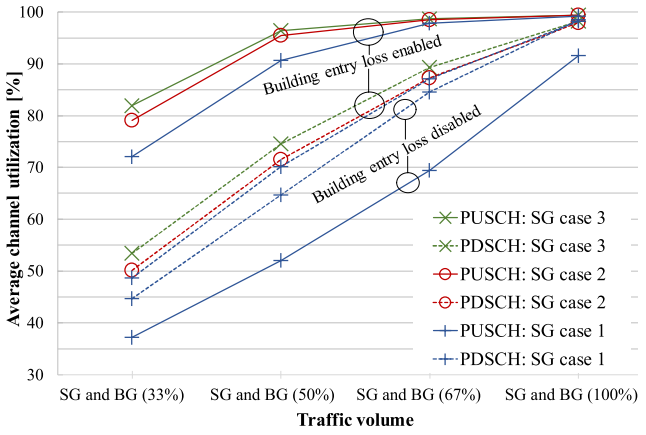


**FIGURE 6.** Average channel utilizations of PUSCH and PDSCH in percentages.

SG and BG (67%), the throughputs are clearly below the loads. This occurs because some of the generated application traffic cannot be delivered due to the lack of network capacity. Based on the theory [23], the maximum throughput is 36.7 Mb/s when utilizing all the resource blocks (50) on a 10 MHz bandwidth and the highest MCS index number (28). The DL traffic load, generated on an application layer, is with the different SG cases approximately from 33.25 to 33.77 Mb/s that is about 90% of the theoretical maximum throughput. The capacity of the UL channel is worse than the DL channel capacity, because lower MCS indexes have to be used due to the limited UE transmission powers. The lower MCS index increases the traffic by applying a lower modulation and using more error correction code. Thus, the network capacity starts to limit the amount of delivered traffic with an average UL traffic load (from 8.79 to 9.19 Mb/s) that is significantly lower than the DL load.

With the traffic volume, SG and BG (67%), the percentage values of the delivered traffic (throughput divided by the load) are approximately 91.2, 92.5, and 89.5% in DL, and approximately 91.8, 88.9, and 87.7% in UL direction in the SG cases 1, 2, and 3, respectively. It can be calculated that the percentage value of the delivered DL traffic is slightly (1.3%) higher in the SG case 2 than in 1, even though the SG case 2 generates ten times more SG traffic in DL direction than SG case 1. This occurs, because BG traffics are randomly generated and their amount may dominate the small SG traffic volume variations between the different SG cases. For example, with the traffic volume, SG and BG (67%), the SG case 2 provides a bit (0.06 Mb/s) smaller total DL traffic load than the SG case 1. Thus, it can be concluded that the percentage value of the delivered traffic is dependent on the amount of overall load despite the amount of the SG traffic. With the highest traffic volume, SG and BG (100%), the load is much higher than the throughput, and the network capacity is clearly exceeded. The percentage values of the delivered traffic are from 67.1 to 71% in UL, from 58.8 to 61.7% in DL, and from 60.5 to 63.3% for the total traffic in the different SG cases (lowest values with the SG case 3).

### C. CHANNEL UTILIZATIONS OF PUSCH AND PDSCH

The Fig. 6 shows the average channel utilization of the physical UL shared channel (PUSCH) (solid lines) and the physical DL shared channel (PDSCH) (round dotted lines) [23] as a function of traffic volume in the SG cases 1, 2, and 3. Also, channel utilizations in the SG case 1 without the building entry loss are presented to illustrate the significance of the signal attenuation caused by the walls. In addition to the application traffic, transmitting header and control data consume also the UL and DL channel bandwidths. Even though the amount of SG traffic is low when compared to the amount of BG traffic, the difference between the channel utilizations with the distinct SG cases can be noticed. Increase in PUSCH utilization between the SG cases 1 and 2 is clear, because four times more SG DR (UL) traffic is generated. The SG DR (UL) traffic amount is the same in the SG cases 2 and 3, nevertheless, a notable rise in SG DR control (DL) traffic amount appears to increase also the PUSCH utilization due to the increased amount of UL control traffic such as HARQ acknowledgments. The increase of PDSCH utilization between the SG cases 1 and 2 is lower than between the SG cases 2 and 3, because the SG DR control (DL) traffic increase is three times higher between the cases 2 and 3 than the cases 1 and 2.

When the network capacity starts to limit the traffic delivery (Fig. 5) remarkably with the traffic amount, SG and BG (67%), the average channel utilization (Fig. 6) approaches the maximum value (100%), being 97.8, 98.4, and 98.6% for PUSCH and 87.1, 87.3, and 89.3% for PDSCH in the SG cases 1, 2, and 3, respectively. With the maximum traffic volume, SG and BG (100%), the average channel utilization is from 99.2 to 99.4% for PUSCH and from 98 to 98.2% for PDSCH with the distinct SG cases. When comparing the channel utilizations in the SG case 1 with and without the building entry loss, it could be seen that the UL traffic suffers

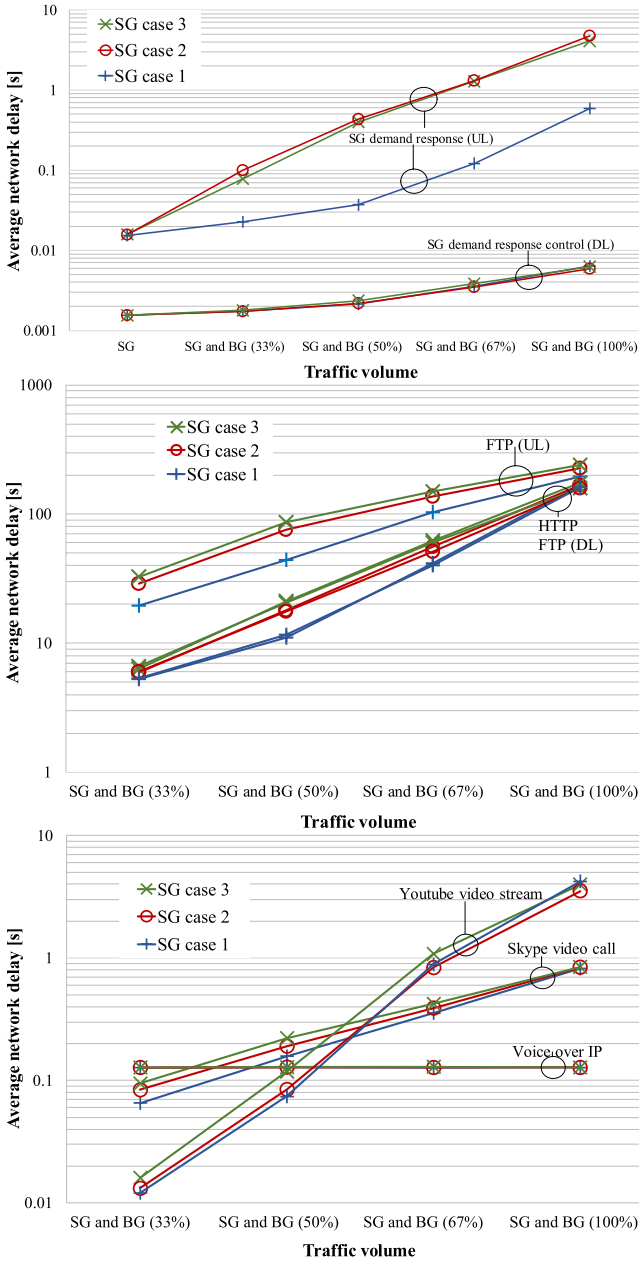


**FIGURE 7.** Average network delays of SG and BG traffic components.

remarkably more from the signal attenuation caused by the walls than the DL traffic. The phenomenon occurs, because lower MCS indexes have to be used in UL direction, due to the limited UE transmission powers, to compensate the increase in signal attenuation. In addition, the building entry loss raises the number of HARQ retransmissions in both directions. The building entry loss appears to increase the channel utilization 34.8, 38.6, 28.4, and 7.7% for PUSCH and 4, 5.5, 2.6, and 0% for PDSCH for the traffic volumes: SG and BG (33, 50, 67, and 100%), respectively.

### D. NETWORK DELAYS OF TRAFFIC COMPONENTS

The Fig. 7 shows the average network delays of SG and BG traffic components as a function of traffic volume in the SG cases 1, 2, and 3. The delays of the SG traffic components are rising when the BG traffic volume is increased by steps from 0 to 100%. When also the BG traffic is generated in the network, the SG DR (UL) traffic delay is remarkably higher in the SG cases 2 and 3 than in the SG case 1. The delay difference occurs, because SG DR (UL) traffic is four times higher in the SG cases 2 and 3 than in the SG case 1. The difference between the delay values among the SG cases 1 and 2 or 3 even increases when the BG traffic volume is increased. The differences between the SG cases 1 and 2 are 0.076, 0.397, 1.188, and 4.182 s with the BG traffic volumes (33, 50, 67, and 100%), respectively. The average network delays of SG DR (UL) traffic, are clearly above the packet generation interval (1 s) in the SG cases 2 and 3 with the BG traffic volumes (67 and 100%), being about 1.3 s with the second highest and more than 4.1 s with the highest BG traffic volume. Higher average network delays than the packet generation interval may lead to congestion in the RLC buffer and further increase the delays and the packet drops. The same amount of SG DR (UL) traffic is generated in the SG cases 2 and 3. However, the SG DR (UL) traffic delays are a bit higher in the SG case 2 than in 3 due to the random BG traffic generation. The differences between the delays of SG DR control (DL) traffics with the different SG cases are extremely low (less than a millisecond). The highest average network delay value for SG DR (UL) traffic is 4.769 s and for SG DR (DL) control traffic is 0.006 s.

The most BG traffic components seem to have a significant increase in the average network delays when the BG traffic volume is increased. As an exception, the average network delay of the voice over IP traffic component stays approximately constant (0.127 - 0.13 s) with all the traffic volumes, because it applies the QoS class of highest priority and the volume of the traffic is relatively low. Skype video call application utilizes a QoS class with GBR that is 1.5 Mb/s in UL and 1.5 Mb/s in DL (in total 3 Mb/s). However, the generated Skype video call traffic amount is above the GBR even with the lowest traffic volume, SG and BG (33%). Thus, the delay increases because channel capacity is scheduled in non-GBR manner for the traffic that cannot be delivered utilizing GBR. The average network delay values of video traffic components with low packet sizes, but relatively high traffic volume, are from 0.012 to 4.218 s for Youtube video stream and from 0.065 to 0.847 s for Skype video call. The average network delay values of BG traffic components with large files are from 19.7 to 240.4 s for FTP (UL), from 5.3 to 174.4 s for FTP (DL), and from 5.3 to 160.2 s for HTTP.

The more a SG case generates traffic the higher increase can be noticed in delays of all the other BG traffic components than voice over IP. Particularly, the distinct hindrance can be seen in delays of FTP and HTTP when the SG DR (UL) traffic amount is four times higher and the SG DR control (DL) traffic amount is ten times higher in the SG case 2 than in 1. With the three lowest BG traffic volumes (33, 50, 67%), the differences between the average network delays of the SG cases 1 and 2 are from 9.17 to 33.2 s for FTP (UL),

from 0.631 to 14.19 s for FTP (DL), and from 0.705 to 10.97 s for HTTP. The differences are larger with a higher BG traffic volume. Solely the SG DR control (DL) traffic amount is increased between the SG cases 2 and 3. However, the thirty times higher SG DR control (DL) traffic amount increases the average network delays of FTP (UL), causing the differences between the delays that are from 3.92 to 14 s. This occurs because a notable rise in SG DR control (DL) traffic amount appears to increase also the UL channel utilization due to the increased amount of UL control traffic.

The increase of SG DR control (DL) traffic volume appears to cause hindrance particularly for Youtube video stream that is fully transmitted in DL direction. The difference between the average network delays of Youtube video stream traffic between the SG cases 1 and 2, with the two lowest BG traffic volumes (33 and 50%), is 0.001 and 0.01 s, respectively. The higher SG DR control (DL) traffic amount in the SG case 3 than in 2, with the two lowest BG traffic volumes, caused 0.003 and 0.034 s higher average network delay values for Youtube video stream. With the two highest BG traffic volumes (67 and 100%), the RLC buffer capacity was exceeded and dropping of packets had the stronger influence for Youtube video stream delays than the variation of SG traffic amount between the distinct SG cases. Thus, an SG case with the higher traffic amount did not necessarily lead to the higher delays for Youtube video stream. Skype video call traffic was transmitted equally in both directions having a bit higher increase in average network delays, from 0.017 to 0.035 s, when SG DR traffic volume was increased in both directions (between the SG cases 1 and 2) than when only the SG DR control (DL) traffic was raised (between the SG cases 2 and 3) and the delay differences were from 0.009 to 0.033 s. With the highest BG traffic volume (100%), the SG DR control (DL) traffic portion of the total DL traffic was quite low (at most 1.2%), and the effect that a higher SG traffic amount causes more increase for delays could be seen only for the BG traffic components that were transmitted fully or partially in UL direction (Skype video call and FTP(UL)).

### E. PACKET DELIVERY RATIOS OF TRAFFIC COMPONENTS

The peak loads, the minimum/maximum/average values of network delays, and the packet delivery ratios (PDRs) over multiple instantiations of the topology are presented in the Table 3. With the two lowest BG traffic volumes (33 and 50%), PDRs of all the SG traffic components are 100%. With the two highest BG traffic volumes (67 and 100%) SG DR control (DL) traffic still obtains PDRs of 100% in all the SG cases. The SG DR (UL) traffic maintains also the PDRs of 100% in the SG case 1. When the SG DR (UL) traffic volume is four times higher in the SG cases 2 and 3, there occur some hindrance for the packet delivery, the PDRs are 99.8 and 99.7% with the second highest and 99.2 and 90% with the highest BG traffic volume. The reduced PDR may cause inaccuracy for DR applications. In the SG case 2, the SG server would not able to apply all the instantaneous energy usage updates, generated by RTUs, to produce adjustments for controlling the local energy production. In the SG case 3, a high-intensity load balancing may have some imprecision for the same reason of not having all the input data.

When observing the BG traffic components, usually increasing the SG traffic volume causes a little or no decrease for the PDRs of the BG traffic components. In general, PDRs of the BG traffic components decrease when the BG traffic volume is increased. However, PDRs of voice over IP stay at 100 or 99.9% with all the traffic volumes due to the relatively low traffic amount (in total less than 1 Mb/s) and the QoS class of highest priority. The average channel utilization (Fig. 6, building entry loss enabled) with the lowest BG traffic volume (33%) is relatively small for the DL channel (about from 49 to 53% for PDSCH) and already quite high for the UL channel (about from 72 to 82% for PUSCH). The BG traffics that are fully transmitted in DL direction (Youtube video stream and HTTP) have PDRs of 100% with the lowest BG traffic volume in all the SG cases. The four times higher SG DR (UL) traffic volume in the SG cases 2 and 3 than in the SG case 1 causes a bit lower PDR values for the BG traffic components that are equally transmitted in both directions (UL and DL). The PDRs are 98.7 and 97.7% for Skype video call and 99.9 and 99.7% for FTP, in the SG case 1 and in the SG cases 2 and 3, respectively.

With the BG traffic volume (50%), the average channel utilization is approximately from 91 to 97% for PUSCH and from 70 to 75% for PDSCH. Now also the BG traffics that are transmitted fully in DL direction have some decrease in PDRs that are from 99.8 to 99.9% for Youtube video stream and from 97.1 to 99.7% for HTTP. The network capacity is exceeded by the two highest BG traffic volumes (67 and 100%), and the PDR values collapsed for the BG traffic components that applied a QoS class without GBR (FTP, Youtube video stream, and HTTP). Thus, the PDRs were from 75 to 94.6% with the second highest and from 32.2 to 69.9% with the highest BG traffic volume. The Skype video call applied a QoS class with GBR and the PDRs stayed approximately on a same level (at most 2.1% difference) with all the traffic volumes, even though the GBR was clearly below the amount of generated traffic.

### F. CAUSES FOR PACKET LOSSES

When inspecting the causes for the decreased PDR values, a couple of reasons were found why some packets were generated on an application layer but not received by a destination node. Firstly, we noticed that HARQ retransmissions occurred, but the cases in which the maximum number of retransmission attempts (3) exceeded did occur very rarely. Thus, HARQ packet drops did not make significant hindrance to the PDRs. In addition, RLC retransmissions that were enabled for SG traffic components to be used after exceeding the maximum number of HARQ retransmissions would not be necessary.

The simulator problem that caused missed packets was the high network delay. For example, with the highest BG traffic

**TABLE 3.** [Peak loads in megabits per second], minimum/maximum/average values of the network delays in seconds, and (packet delivery ratios in percentages).

| Traffic component [peak load] | SG case | SG and BG (33%) traffic | SG and BG (50%) traffic | SG and BG (67%) traffic | SG and BG (100%) traffic |
|---|---|---|---|---|---|
| SG DR (UL) [0.175 Mb/s] | 1 | 0.005/12.43/**0.023** s (**100%**) | 0.005/15.83/**0.037** s (**100%**) | 0.005/18.4/**0.121** s (**100%**) | 0.005/29.03/**0.587** s (**100%**) |
| SG DR (UL) [0.6 Mb/s] | 2 | 0.005/25.27/**0.099** s (**100%**) | 0.005/39.53/**0.434** s (**100%**) | 0.005/147.7/**1.309** s (**99.8%**) | 0.005/330.9/**4.769** s (**99.2%**) |
| SG DR (UL) [0.6 Mb/s] | 3 | 0.005/24.77/**0.078** s (**100%**) | 0.005/58.87/**0.401** s (**100%**) | 0.005/153.3/**1.293** s (**99.7%**) | 0.005/308.5/**4.129** s (**99%**) |
| SG DR control (DL) [0.0072 Mb/s] | 1 | 0.001/0.013/**0.002** (**100%**) | 0.001/0.015/**0.002** s (**100%**) | 0.001/0.016/**0.004** s (**100%**) | 0.001/0.02/**0.006** s (**100%**) |
| SG DR control (DL) [0.0312 Mb/s] | 2 | 0.001/0.02/**0.002** s (**100%**) | 0.001/0.022/**0.002** s (**100%**) | 0.001/0.022/**0.003** s (**100%**) | 0.001/0.027/**0.006** s (**100%**) |
| SG DR control (DL) [0.6 Mb/s] | 3 | 0.001/0.03/**0.002** s (**100%**) | 0.001/0.031/**0.002** s (**100%**) | 0.001/0.03/**0.004** s (**100%**) | 0.001/0.03/**0.006** s (**100%**) |
| Voice over IP [1.61, 1.61, 1.57, 1.63 Mb/s] | 1 | 0.082/1.207/**0.127** s (**100%**) | 0.082/7.218/**0.128** s (**99.9%**) | 0.081/2.268/**0.127** s (**100%**) | 0.081/2.863/**0.128** s (**100%**) |
| | 2 | 0.082/0.696/**0.127** s (**100%**) | 0.081/4.678/**0.128** s (**99.9%**) | 0.082/7.009/**0.128** s (**100%**) | 0.081/6.673/**0.128** s (**100%**) |
| | 3 | 0.082/1.423/**0.127** s (**100%**) | 0.082/7.178/**0.129** s (**99.9%**) | 0.081/28.44/**0.13** s (**99.9%**) | 0.081/2.452/**0.128** s (**100%**) |
| Skype video call [19.03, 22.86, 24.73, 28.5 Mb/s] | 1 | 0.001/21.68/**0.065** s (**98.7%**) | 0.001/27.75/**0.158** s (**97.7%**) | 0.001/21.75/**0.355** s (**97.1%**) | 0.001/29.49/**0.821** s (**97%**) |
| | 2 | 0.001/26.16/**0.084** s (**97.7%**) | 0.001/31.45/**0.19** s (**97%**) | 0.001/40.47/**0.39** s (**96.8%**) | 0.001/37.7/**0.838** s (**97.1%**) |
| | 3 | 0.001/26.98/**0.095** s (**97.7%**) | 0.001/28.38/**0.221** s (**96.8%**) | 0.001/50.69/**0.423** s (**96.6%**) | 0.001/24.073/**0.847** s (**96.9%**) |
| FTP (UL) FTP (DL) [69.6, 92.81, 116, 139.2 Mb/s] | 1 | 3.797/449.9/**19.67** s 3.583/192.5/**5.289** s (**99.9%**) | 3.822/589.7/**44.29** s 3.59/447.6/**11.08** s (**99%**) | 3.793/831.4/**103.3** s 3.592/650.9/**41.81** s (**84.9%**) | 3.822/842.7/**194.6** s 3.601/810.7/**166.9** s (**42.7%**) |
| | 2 | 3.997/567.6/**28.84** s 3.594/264.9/**5.92** s (**99.7%**) | 3.95/673.4/**75.84** s 3.594/555.9/**18.07** s (**96.2%**) | 3.993/814/**136.5** s 3.602/648.2/**56** s (**77.6%**) | 4.022/810.3/**226.4** s 3.611/828.3/**166.9** s (**35.1%**) |
| | 3 | 4.009/454.6/**32.76** s 3.61/213.4/**6.29** s (**99.7%**) | 4.129/689.3/**85.94** s 3.604/510/**21.02** s (**94%**) | 4.138/830.6/**149.5** s 3.622/686.7/**62.35** s (**75%**) | 4.022/848.5/**240.4** s 3.626/852.3/**174.4** s (**32.2%**) |
| Youtube video stream [24, 27.2, 37.3, 51.2 Mb/s] | 1 | 0.002/22.02/**0.012** s (**100%**) | 0.002/58.47/**0.074** s (**99.9%**) | 0.002/55.78/**0.889** s (**94.2%**) | 0.002/59.9/**4.218** s (**65%**) |
| | 2 | 0.002/29.46/**0.013** s (**100%**) | 0.002/59.32/**0.084** s (**99.9%**) | 0.002/59.5/**0.838** s (**94.6%**) | 0.002/59.18/**3.52** s (**69.9%**) |
| | 3 | 0.002/29.32/**0.016** s (**100%**) | 0.002/46.15/**0.118** s (**99.8%**) | 0.002/58.07/**1.08** s (**92.9%**) | 0.002/61.63/**3.968** s (**66.4%**) |
| HTTP [72, 96, 120, 144 Mb/s] | 1 | 3.707/200.3/**5.323** s (**100%**) | 3.729/404.2/**11.68** s (**99.7%**) | 3.718/787.4/**40.24** s (**90.1%**) | 3.777/846.8/**160.2** s (**45%**) |
| | 2 | 3.719/198.9/**6.028** s (**100%**) | 3.742/555.6/**17.59** s (**98.3%**) | 3.718/730.9/**51.21** s (**87.4%**) | 3.756/839.8/**159** s (**39.2%**) |
| | 3 | 3.744/296.8/**6.641** s (**100%**) | 3.752/529.5/**20.47** s (**97.1%**) | 3.766/820/**59.88** s (**84.7%**) | 3.801/851.3/**159.5** s (**34.6%**) |

value (100%), SG DR (UL) traffic obtained average network delay values from 4 to 5 s in the SG cases 2 and 3, and the maximum network delay values were more than 300 s. The traffic was generated during the last 15 min of the 20 min simulation time, and some of the last packets with high delay might not be received before the simulation end time. In addition, BG traffic applications with small packets applying UDP (voice over IP, Skype video call, and Youtube video stream) had constant application durations with random start times selected to finish the application before the end of a simulation run. However, some packets with high delay might not be received prior to the simulation end time and are considered as lost packets. The traffic components with large files (HTTP and FTP) applied TCP that provided a reliable packet delivery. HTTP and FTP packets were not generated during the last 30 s of a simulation run to prevent unnecessary packet losses. However, the lack of network capacity caused remarkably high network delays and some of these large packets were not delivered successfully. We tested that all the TCP traffic (HTTP and FTP) could be finally delivered successfully if the simulation time would be extended without the other traffic applications and the network congestion.

The computing problem that inflicted packet losses was exceeding the maximum RLC buffer size of 1500 packets. Due to the computer performance limitations, it was not possible to perform simulations within total of 1680 nodes (930 UE and 750 RTUs). Thus, the simulations were performed by locating one node for UE traffic and one node for RTU traffic per each cluster to communicate the traffic of 31 UE and 25 RTUs, and the amount of traffic generated

**TABLE 4.** [Peak loads in megabits per second], minimum/maximum/average values of the network delays in seconds, and (packet delivery ratios in percentages) when the maximum RLC buffer size was increased.

| Traffic component [peak load] | SG case | SG and BG (100%) traffic |
|---|---|---|
| SG DR (UL) [0.6 Mb/s] | 3 | 0.005/474.9/**4.088** s (**99.8%**) |
| SG DR control (DL) [0.6 Mb/s] | 3 | 0.001/0.035/**0.008** s (**100%**) |
| Voice over IP [1.59 Mb/s] | 3 | 0.082/11.21/**0.129** s (**99.9%**) |
| Skype video call [28.53 Mb/s] | 3 | 0.001/223.2/**0.935** s (**97.5%**) |
| FTP (UL) FTP (DL) [139.2 Mb/s] | 3 | 4.022/884.4/**210.1** s 3.626/814.5/**141.8** s (**30.7%**) |
| Youtube video stream [52.8 Mb/s] | 3 | 0.002/420.8/**53.48** s (**93.4%**) |
| HTTP [120 Mb/s] | 3 | 3.801/855.6/**139.7** s (**34.8%**) |

**TABLE 5.** [Peak loads in megabits per second], minimum/maximum/average values of the network delays in seconds, and (packet delivery ratios in percentages) when the maximum RLC buffer size was increased and SG traffic generation ended 1 min prior to the simulation end time.

| Traffic component [peak load] | SG case | SG and BG (100%) traffic |
|---|---|---|
| SG DR (UL) [0.6 Mb/s] | 3 | 0.005/474.9/**4.321** s (**99.9%**) |
| SG DR control (DL) [0.6 Mb/s] | 3 | 0.001/0.035/**0.008** s (**100%**) |
| Voice over IP [1.59 Mb/s] | 3 | 0.082/11.21/**0.129** s (**99.9%**) |
| Skype video call [28.53 Mb/s] | 3 | 0.001/223.2/**0.934** s (**97.5%**) |
| FTP (UL) FTP (DL) [139.2 Mb/s] | 3 | 4.022/880.4/**214.3** s 3.626/814/**143.5** s (**31.1%**) |
| Youtube video stream [52.8 Mb/s] | 3 | 0.002/423.1/**53.52** s (**93.6%**) |
| HTTP [120 Mb/s] | 3 | 3.801/855.3/**141** s (**34.9%**) |

by each node increased remarkably. Generated packets were dropped when the RLC buffer was full. The effect of dropping packets instead of inserting into RLC buffer was particularly notable for the Youtube video stream that generated small packets with frequent intervals and applied a QoS class without GBR. When the PDRs of Youtube video stream dropped dramatically with the highest BG traffic value, the network delays were already excessively high (the average value was about 4 s and the maximum value was approximately 1 min) for video streaming. Each Youtube video stream generated 24 packets per second and there may be multiple concurrently operating applications per UE. The maximum RLC buffer size appears to limit the maximum delay for the Youtube video stream. The maximum delay was slightly lower than the time duration that could be calculated by dividing the maximum RLC buffer size with the number of packets generated per second, $1500 / 24 = 62.5$ s.

### G. ELIMINATING SIMULATOR AND COMPUTATION RESTRICTIONS

The most congested network situation, SG and BG (100%) in the SG case 3, was simulated once more to investigate if the network would provide better performance results for SG traffic components without the simulator and computing restrictions. The maximum RLC buffer size was increased for all the nodes to be 37500 packets (25 multiplied with 1500 packets) to correspond to the number of RTUs in a cluster. The peak loads, the minimum/maximum/average values of network delays, and the PDRs are presented in the Table 4. When comparing the new results with the previous results presented in the Table 3, it can be seen that the PDR of SG DR (UL) traffic increased from 99 to 99.8%. The average network delay decreased slightly from 4.129 to 4.088 s, but the maximum network delay increased from 308.5 to 474.9 s due to the capability of storing more packets into RLC buffers. The average network delay of SG DR control (DL) traffic increased slightly from 0.006 to 0.008 s. The highest difference in the performance was induced for the Youtube video stream traffic that increased the PDR from 66.4 to 93.4%. However, the average network delay increased from 3.968 to 53.48 s being far too high for video streaming. PDR of Skype video call increased a bit from 96.9 to 97.5% while the higher RLC buffer size allowed the maximum network delay value to grow from 24.07 to 223.2 s. On the contrary, the traffic applications with large packets (FTP and HTTP) had from 20 to 30 s decrease in average network delays, because the amount of generated FTP traffic decreased from 11.6 to 8.1 Mb/s and the amount of HTTP traffic from 11.9 to 8.4 Mb/s. This occurred, because less TCP traffic connections were able to be established while UDP traffic applications, particularly Youtube video stream, occupied more DL channel capacity.

With the increased RLC buffer size, 0.2% of the SG DR (UL) packets were still not received. Thus, the most congested network situation was simulated when, in addition to increasing the maximum RLC buffer size, also the SG traffic generation was stopped one minute before the simulation end time to alleviate the delivery of SG packets with a high delay. The simulation results are presented in the Table 5. When comparing these with the previous results of the Table 4, it can be seen that the PDR of SG DR (UL) traffic increased from 99.8 to 99.9%. The average network delay of SG DR (UL) traffic increased from 4.088 to 4.321 s, because about 0.1% of packets with relatively high delay were received during the last minute of simulation time. However, 0.1% of the SG DR (UL) packets were still not received, because the maximum network delay (475 s) was clearly above the one minute that was the time at the end of a simulation run without new SG traffic generations. Even though the PDR was close to 100%, the average network delay of SG DR (UL) traffic was clearly above the packet generation interval of SG DR control (DL) traffic, 1 s. Thus, the energy usage updates that were generated by the RTUs and received by the SG server with a delay higher than the adjustment period were useless

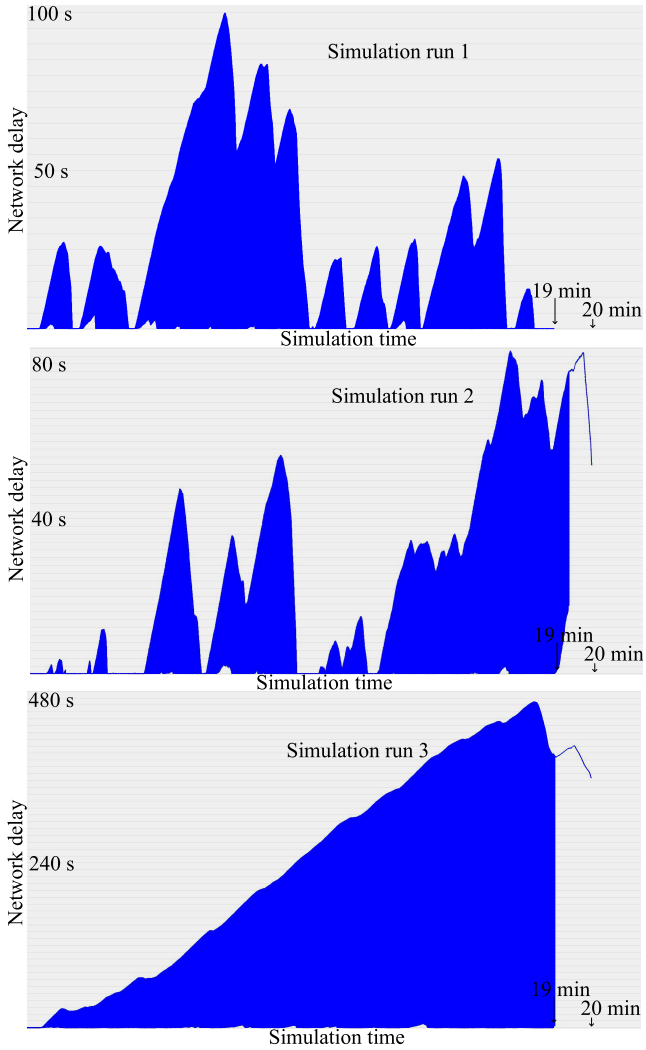


**FIGURE 8.** Network delays of SG DR (UL) traffic (SG and BG (100%) in the SG case 3) with the increased maximum RLC buffer size when SG traffic generation is stopped one minute prior to the simulation end time.

for high-intensity load balancing. It could be observed that PDRs of the BG traffic components using a QoS class without GBR (FTP, Youtube video stream, and HTTP) had a bit better PDR values than previously, because the last minute of the 20 min simulation time was performed without SG traffic generations.

The Fig. 8 shows network delay values of all received SG DR (UL) packets as a function of simulation time, separately with three distinct simulation runs, applying the highest traffic volume, SG and BG (100%) in the SG case 3. The figure presents the simulation time from 5 to 20 min, and the SG traffic generation is stopped after the 19 min of simulation time. In addition, the increased maximum RLC buffer size is applied. The simulation runs were selected to present three different situations of delay behavior. The delay differs highly between the distinct simulation runs, because the network capacity is exceed and the amount of obtained channel resources may vary. Based on the topmost part of the figure (simulation run 1), it can be seen that the delays increase for some periods of time due to the lack of channel capacity, but finally a sufficient amount of capacity is obtained and the traffic is transmitted successfully. At the end of the simulation run, the network delays are at the low level and no packet receptions occur after the 19 min of simulation time. The obtained PDR is 100%. In the middle part of the figure (simulation run 2), there are high delay values at the end of the simulation run, because some SG DR (UL) packets are transmitted during the last minute. The obtained PDR is still 100%. The lowest part of the figure (simulation run 3) shows a simulation run in which SG DR (UL) traffic has difficulties to obtain a sufficient amount of capacity during the whole time and network delays increase linearly until the SG traffic generation ends at the 19 min of simulation time. During the last minute, some SG DR (UL) packets are transmitted, but there are such a high number of packets in RLC buffers that all pending packets cannot be delivered. Thus, the obtained PDR is solely 98.8%.

## V. DISCUSSION

### A. SIMULATOR AND COMPUTATION RESTRICTIONS

The simulations of previous conference papers and of this paper were performed using the same topology. The topology contained 930 UE and 750 RTUs equally distributed into 30 clusters. Due to the computer performance limitations, it was not possible to perform simulations within total of 1680 nodes. Thus, the simulations were performed locating one node for UE traffic and one node for RTU traffic per each cluster to communicate the traffic of 31 UE and 25 RTUs. The amount of generated application load was the same, even though the number of nodes was reduced. A slight inaccuracy may be caused by the decreased amount of control traffic delivered in PUCCH and physical DL control channel (PDCCH) [23]. However, this research did not focus to the traffic transmitted in these control channels.

One RLC buffer was applied for each node communicating the traffic of 31 UE or 25 RTUs in UL direction. Also, one RLC buffer was used by the eNB per each destination node for DL packet transmissions. Because the traffic communicated by various UE or RTUs was modeled by a single node, there occurred some packet drops due to the exceeding of the maximum number of packets in an RLC buffer (1500). Thus, some decrease in PDR values were caused particularly for traffic applications with frequent packet generations when the network load was high. Simulations with the highest traffic volume when using increased maximum RLC buffer size were performed. The results illustrated that the PDRs of SG DR (UL) traffic increased from 99 to 99.8% causing some increase in maximum network delays (from 309 to 475 s). Thus, it could be concluded that the improved PDR was consequence of the reception of packets with high delay. For example, the maximum network delay of Youtube video stream increased from 62 to 421 s while the PDR improved from 64.4 to 93.6%.

At the end of a simulation run, there may be some packets with such high delay that they cannot be received prior to the

simulation end time. It was illustrated by the simulations that 0.2% of the SG DR (UL) packets were not received before the simulation end time with the highest traffic volume. With one minute excess time without SG traffic generation, half of these packets were received, but the other half of the packets were still not received due to the high delay. The traffic applications using TCP (FTP and HTTP) for reliable packet delivery had the decreased PDRs due to the lack of network capacity for transmissions of relatively large packets. However, all TCP traffic could be delivered successfully when the simulation time was extended without new packet generations, i.e. when there was no lack of network capacity anymore. Obviously, applying TCP for SG DR traffic is not reasonable due to the significant increase of control traffic overhead for relatively small packets.

### B. LTE PARAMETERS

The most LTE parameters were the same for the previous conference papers and for this paper. For example, HARQ retransmissions were equally applied for all the traffic types, but RLC retransmissions were enabled solely for the SG traffics. However, RLC retransmissions would not be necessary for the SG traffics, because the maximum number of HARQ retransmissions exceeded rarely. In the two first conference papers [12], [13], the PDCP was not enabled and uncompressed IP related headers added some overhead traffic in the simulations. In this and the previous paper [15], the PDCP was applied to compress the headers. However, the typical application traffic (BG traffic) amount was significantly higher (from 22.2 to 60.5 Mb/s) in this and the previous paper [15] than in the two first papers [12], [13] (10.5 Mb/s). The higher volume of the typical traffic was applied, because the volume of the traffic in a cellular network has increased remarkably during the last years and will continue growing in the future [32]. In addition, the intention was to model a situation in which the network capacity was exceeded while the UL traffic was about 21% of the total traffic being at the realistic maximum level.

DRX conserves the battery by turning off the receiver of an RTU or a UE for some periods of time and may cause some increase in DL traffic delays. Applying DRX was not crucial in this paper, because RTUs were assumed to be plugged into the electrical network, i.e. the battery life of an LTE RTU would not be sufficient with or without DRX. The DRX capability was enabled solely in the previous conference paper [15]. The applied DRX parameters are presented in Table 1. Two distinct DRX cycles were used in the simulations. The short DRX cycle timer defines the total length of the short DRX cycle. The long DRX cycle multiplication factor defines the long DRX cycle length as a multiple of the short DRX cycle length. At the start of the each DRX cycle, on duration timer counts the time in which the UE scans the PDCCH to check if it has any upcoming DL transmissions from the eNB. The inactivity timer is activated to continue the receiver on time if PDCCH data is received, and a new DL reception restarts the timer. After the inactivity timer has expired there starts a new short DRX cycle. If the on duration timer has expired, the receiver will be turned off for the sleep period of the short DRX cycle. When the receiver is turned off, the cycle can be broken only by arrival of higher layer UL data. The long DRX cycles immediately follow the short DRX cycle if the short cycle was not broken. If a short or a long DRX cycle was broken and the DRX resumes, the short DRX cycle is employed first. The retransmission timer counts the time that UE waits to receive a DL retransmission packet after the HARQ round trip timer expires since the last transmission. This time is granted to the UE because DL retransmissions are asynchronous and can be scheduled unpredictably depending upon the availability of resources.

DRX was disabled in this paper, because it may cause some inaccuracy for the DL traffic delays due to the modeling of multiple RTUs or UE by a single node. To be precise, the average DL traffic delay is increased less by the DRX, because more UL traffic is generated per node to break the DRX cycle and to turn on the receiver. Nevertheless, when comparing the maximum network delay results of SG DR (DL) traffic in the SG case 2 of this paper (from 20 to 27 ms) with the results of the paper [15] (from 139 to 201 ms), the effect of DRX for increasing the delays can be illustrated.

### C. PREVIOUS WORK

In [12], the authors illustrated that a public LTE network is suitable for SG automatic meter usage without causing significant hindrance to typical public LTE traffic. Based on the simulation results, the regular SG monitoring traffic amount is low (2.6 kb/s in UL and 0.5 kb/s in DL) and does not cause significant effect for the network performance. The high instant traffic generated during critical emergency events can be delivered with 100% probability by adding the artificial, [0, 1] s random delay for packet transmissions, or by applying a hybrid sensor-LTE network.

In [13], SG DR scenarios were simulated in an LTE and a hybrid sensor (IEEE 802.15.4)-LTE networks. Higher MCS indexes were applied and the number of HARQ retransmissions was reduced for SG traffic in the hybrid network, because the antennas of CLHs were located outside and there were no pathloss caused by the walls between the CLHs and the eNB. The hybrid network appeared to have a lower impact on the typical public LTE traffic due to the lower overhead of SG traffic (higher modulation, less error correction code, and less retransmissions). For the same reason, the SG traffic delay in UL direction was lower in the hybrid network. On the other hand, PDR values were higher (at least 99%) in the LTE network, because the sensor interface of the hybrid network caused some packet collisions due to the applied MAC protocol (CSMA-CA) that used up to three retransmissions. The simulations did not consider the fact that a sensor network is operated on unlicensed frequency bands that may contain additional interference. The LTE network

obtained better results in security than the hybrid network according to the feasibility assessment presented in [16]. The hybrid network induced better results in the cost metric due to the reduced expenses in the subscriptions and communication devices. However, the LTE network appears to be the better solution for SG traffic communications due to the reliability and the security in packet delivery. To reduce the overhead of SG traffic and at the same time decrease the hindrance for the typical traffic, it would be beneficial to locate the antennas of smart meters in an intelligent manner to obtain optimal propagation paths to the base station.

In [14], the authors have proposed an ad hoc mode for the LTE-Advanced UE to overcome issues relating to lack of base station connectivity. For example, an RTU considered as a UE may be installed in a basement or in buildings that have high penetration losses, or even a base station may be malfunctioning. The purpose was to research the performance of the solution for SG DR communication in an ad hoc radio propagation environment using network simulations and mathematical analysis. Particularly, the PDRs and the delays with distinct transmission powers and different numbers of transmission attempts were observed. The receiver applied HARQ with chase combining to combine the bits from the current and the previous transmission attempt to achieve a better probability for a successful packet reception. The proposed solution applied mostly the same physical layer characteristics as NB-IoT [33] using a single resource block and a UL transmitter. Thus, the solution and the results may be useful in NB-IoT network planning for selecting transmission powers and numbers of repetition transmissions that may improve the packet delivery in challenging radio propagation environments.

In the previous paper [15], the authors have researched the influence of a highly loaded public LTE network for the SG DR traffic delivery when the effects of QoS class selection for SG DR traffic components were researched. Lowering the QoS of the RTUs that transmitted in UL direction was not reasonable, because the SG DR (UL) traffic delay increased and the PDRs decreased remarkably already with the lowest typical traffic volume. The QoS could be lowered for the SG server that transmitted SG DR control traffic in DL direction, but no notable improvements were achieved for the typical LTE traffic performance.

### D. CURRENT WORK

In this paper, the simulations of [15] were refined. The communications performance with the three distinct DR applications (different SG cases) was researched instead of observing the effects of QoS class selections. The lowest amount of SG DR traffic was generated in the SG case 1 using packet generation intervals of 4 s in UL and 5 min in DL for each RTU. The SG case 1 induced PDRs of 100%, and at most 29 s maximum and 0.6 s average network delays, for the SG traffics with all the BG traffic volumes. The SG cases 2 and 3 generated packets with intervals of 1 s in UL and 30 s (SG case 2) and 1 s (SG case 3) in DL. The SG cases 2 and 3 caused a significant increase for the maximum delay values of SG DR (UL) traffic and a notable hindrance for the BG traffic components with the three highest BG traffic volumes (50, 67, and 100%). The increased hindrance for the most BG traffic components could be seen when the SG DR traffic volume was raised between the different SG cases. As an exception, voice over IP traffic that applied the QoS class of highest priority was not harmed by the any SG case.

The simulation results illustrated that the SG DR (UL) traffic could be transmitted in all the SG cases with at least 99% PDR even when the network capacity was clearly exceeded. The minimum PDR value of SG DR (UL) traffic could be improved from 99 to 99.8% by increasing the RLC buffer size. However, the increased RLC buffer size allowed the transmission of more packets with excessively high delay. This can be illustrated by the maximum delay values that were 331 s with the initial RLC buffer size and 475 s with the increased RLC buffer size. SG DR control (DL) traffic could be delivered with 100% probability with all the different traffic volumes while maintaining the maximum delay of 31 ms. The satisfactory performance for the SG DR traffic components could be maintained due to the constant traffic characteristics and relatively low traffic amount that facilitated the scheduling of a sufficient amount of channel capacity for transmissions.

The most recommended option for the overall network performance would be to generate SG DR traffics according to the SG case 1. The reasonable maximum delay values would be maintained for all the SG DR traffics and hindrance for the typical traffics would be minimized. With the lowest BG traffic volume (33%) in the SG cases 2 and 3, it was possible to maintain the relatively low maximum (below 25.3 s) and average (below 0.1 s) delays for the SG DR (UL) traffic and low hindrance for the BG traffic. Thus, the SG cases 2 and 3 would be suitable DR applications in the shared LTE network with certain conditions; if the BG traffic amount is relatively low, or minimizing the hindrance for the BG traffic is not a priority and the high maximum (up to a few hundreds of seconds) and average (up to 4.8 s) delays of SG DR (UL) traffic are not an issue.

The SG case 1 scenario presented a DR program of spot pricing for balancing out the network load. The communications performance was suitable for this DR program with all the BG traffic volumes. The SG case 2 was modeled as a DR program for enabling local energy production. The average network delays of SG DR (UL) traffic were above the packet generation interval. Obviously, this may lead to congestion in the RLC buffer and further increase the delays and the packet drops. The SG case 3 was modeled as high-intensity load balancing. In this case, the average network delays of SG DR (UL) traffic were above the packet generation intervals of the both, SG DR (UL) and SG DR control (DL) traffics. This may lead to another issue in which the energy usage updates that are generated by the RTUs will be received by the SG server with a delay higher than the adjustment period and are useless for high-intensity load balancing. In the SG

cases 2 and 3, the PDRs are reduced with the two highest BG traffic volumes. Lost packets may cause additional inaccuracy for DR applications. In the SG case 2, the SG server would not be able to apply all the instantaneous energy usage updates, generated by RTUs, to produce adjustments for controlling the local energy production. In the SG case 3, a high-intensity load balancing would have some imprecision for the same reason of not having all the input data.

## VI. CONCLUSION AND THE FUTURE WORK

In this paper, the possibility of delivering distinct SG DR traffics in a highly loaded LTE network is researched. The research results indicated that a public LTE network is suitable for SG communications with certain limitations related to the traffic volume and the radio channel capacity. The packet delivery ratios were at least 99% for SG DR (UL) traffic and 100% for SG DR control (DL) traffic in all the SG cases even when the network capacity was clearly exceeded. However, the SG cases 2 and 3 caused a significant increase for the maximum delay values of SG DR (UL) traffic (up to 331 s) and a notable hindrance for the BG traffic components with the three highest BG traffic volumes.

LTE network coverage is widely available in most countries of the world that facilitates its deployment for SG communications. NB-IoT is another potential cellular-based option for SG communications, but it is still marginally deployed and there is no guarantee of its success among the network operators in the future. Thus, the future work may contain research of NB-IoT network suitability for SG communications. LoRaWAN might be a potential solution for delivering low SG traffic volumes (e.g. AMR traffic) in large areas due to the high transmission distances [34]. In the future work, the LoRaWAN may be further optimized and improved to increase the reliability and the capacity for SG communications.

## REFERENCES

[1] V. C. Gungor, D. Sahin, T. Kocak, S. Ergut, C. Buccella, C. Cecati, and G. P. Hancke, "A survey on smart grid potential applications and communication requirements," *IEEE Trans Ind. Informat.*, vol. 9, no. 1, pp. 28–42, Feb. 2013.

[2] F. Aalamifar, H. S. Hassanein, and G. Takahara, "Viability of powerline communication for the smart grid," in *Proc. 26th Biennial Symp. Commun. (QBSC)*, May 2012, pp. 19–23.

[3] *Smart Energy Grids and Complexity Science*, document EUR 25626 EN, Joint Research Centre Institute for Energy and Transport, European Commission, 2012.

[4] D. Devogelaer, J. Duerinck, D. Gusbin, Y. Marenne, W. Nijs, M. Orsini, and M. Pairon, "Towards 100% renewable energy in Belgium by 2050," FPB, ICEDD, VITO, Mol, Belgium, Tech. Rep., Apr. 2013. [Online]. Available: https://energie.wallonie.be/servlet/Repository/130419-backcasting-finalreport.pdf?ID=28161

[5] H. Lund and B. V. Mathiesen, "Energy system analysis of 100% renewable energy systems—The case of denmark in years 2030 and 2050," *Energy*, vol. 34, no. 5, pp. 524–531, May 2009.

[6] B. V. Mathiesen, H. Lund, D. Connolly, H. Wenzel, P. A. Østergaard, B. Möller, S. Nielsen, I. Ridjan, P. Karnøe, K. Sperling, and F. K. Hvelplund, "Smart energy systems for coherent 100% renewable energy and transport solutions," *Appl. Energy*, vol. 145, pp. 139–154, May 2015.

[7] G. Pleßmann, M. Erdmann, M. Hlusiak, and C. Breyer, "Global energy storage demand for a 100% renewable electricity supply," *Energy Procedia*, vol. 46, pp. 22–31, Jan. 2014.

[8] A. Pouttu, J. Haapola, P. Ahokangas, Y. Xu, M. Kopsakangas-Savolainen, E. Porras, J. Matamoros, C. Kalalas, J. Alonso-Zarate, F. D. Gallego, J. M. Martin, G. Deconinck, H. Almasalma, S. Clayes, J. Wu, M. Cheng, F. Li, Z. Zhang, D. Rivas, and S. Casado, "P2P model for distributed energy trading, grid control and ICT for local smart grids," in *Proc. Eur. Conf. Netw. Commun. (EuCNC)*, Jun. 2017, pp. 1–6.

[9] A.-H. Mohsenian-Rad and A. Leon-Garcia, "Optimal residential load control with price prediction in real-time electricity pricing environments," *IEEE Trans. Smart Grid*, vol. 1, no. 2, pp. 120–133, Sep. 2010.

[10] C. Ibars, M. Navarro, and L. Giupponi, "Distributed demand management in smart grid with a congestion game," in *Proc. 1st IEEE Int. Conf. Smart Grid Commun.*, Oct. 2010, pp. 495–500.

[11] A. Molina, A. Gabaldon, J. A. Fuentes, and C. Alvarez, "Implementation and assessment of physically based electrical load models: Application to direct load control residential programmes," *IEE Proc.—Gener., Transmiss. Distrib.*, vol. 150, no. 1, pp. 61–66, Apr. 2003.

[12] J. Markkula and J. Haapola, "Impact of smart grid traffic peak loads on shared LTE network performance," in *Proc. IEEE Int. Conf. Commun. (ICC)*, Jun. 2013, pp. 4046–4051.

[13] J. Markkula and J. Haapola, "LTE and hybrid sensor-LTE network performances in smart grid demand response scenarios," in *Proc. IEEE Int. Conf. Smart Grid Commun. (SmartGridComm)*, Oct. 2013, pp. 187–192.

[14] J. Markkula and J. Haapola, "Ad hoc LTE method for resilient smart grid communications," *Wireless Pers. Commun.*, vol. 98, no. 4, pp. 3355–3375, Oct. 2017.

[15] J. Markkula and J. Haapola, "Impact of shared LTE network high typical traffic loads on smart grid demand response schemes," in *Proc. 3rd Int. Conf. Smart Sustain. Technol. (SpliTech)*, Jun. 2018, pp. 1–6.

[16] J. Haapola, J. Alonso-Zarate, G. Deconinck, H. Almasalma, J. Wu, C. Zhang, E. P. Munoz, F. D. Gallego, S. Ali, C. Kalalas, J. Markkula, N. Rajatheva, A. Pouttu, J. M. M. Rapun, I. Lalaguna, and F. Vazquez-Gallego, "Peer-to-peer energy trading and grid control communications Solutions' feasibility assessment based on key performance indicators," in *Proc. IEEE 87th Veh. Technol. Conf. (VTC Spring)*, Jun. 2018, pp. 1–5.

[17] J. Brown and J. Y. Khan, "Performance comparison of LTE FDD and TDD based smart grid communications networks for uplink biased traffic," in *Proc. IEEE 3rd Int. Conf. Smart Grid Commun. (SmartGridComm)*, Nov. 2012, pp. 276–281.

[18] M. Carlesso, A. Antonopoulos, F. Granelli, and C. Verikoukis, "Uplink scheduling for smart metering and real-time traffic coexistence in LTE networks," in *Proc. IEEE Int. Conf. Commun. (ICC)*, Jun. 2015, pp. 820–825.

[19] C. Karupongsiri, K. S. Munasinghe, and A. Jamalipour, "A novel communication mechanism for smart meter packet transmission on LTE networks," in *Proc. IEEE Int. Conf. Smart Grid Commun. (SmartGridComm)*, Nov. 2016, pp. 122–127.

[20] G. C. Madueno, J. J. Nielsen, D. M. Kim, N. K. Pratas, C. Stefanovic, and P. Popovski, "Assessment of LTE wireless access for monitoring of energy distribution in the smart grid," *IEEE J. Sel. Areas Commun.*, vol. 34, no. 3, pp. 675–688, Mar. 2016.

[21] J. J. Nielsen, H. Ganem, L. Jorguseski, K. Alic, M. Smolnikar, Z. Zhu, N. K. Pratas, M. Golinski, H. Zhang, U. Kuhar, Z. Fan, and A. Svigelj, "Secure real-time monitoring and management of smart distribution grid using shared cellular networks," *IEEE Wireless Commun.*, vol. 24, no. 2, pp. 10–17, Apr. 2017.

[22] *Riverbed*. Accessed: Nov. 27, 2018. [Online]. Available: http://www.riverbed.com

[23] *LTE; Evolved Universal Terrestrial Radio Access (E-UTRA); Physical Layer Procedures*, document TS 36.213, ver. 11.6.0 Rel. 11, 3GPP, 2014, pp. 29–175.

[24] A. Dahlman, S. Parkvall, J. Sköld, and P. Meming, *3G Evolution: HSPA LTE for Mobile Broadband*, 2nd ed. Oxford, MS, USA: Elsevier, 2008, pp. 40–46, 105–117, 131, 470–475, and 488–490.

[25] *Technical Specification Group Radio Access Network; Spatial Channel Model for Multiple Input Multiple Output (MIMO) Simulations*, document TR 25.996, ver. 10.0.0 Rel. 10, 3GPP, 2011, pp. 16–18.

[26] D. Molkdar, "Review on radio propagation into and within buildings," *IEE Proc. H Microw., Antennas Propag.*, vol. 138, no. 1, pp. 61–73, Feb. 1991.

[27] C. R. Anderson and T. S. Rappaport, "In-building wideband partition loss measurements at 2.5 and 60 GHz," *IEEE Trans. Wireless Commun.*, vol. 3, no. 3, pp. 922–928, May 2004.

[28] T. K. Sarkar, Z. Ji, K. Kim, A. Medouri, and M. Salazar-Palma, "A survey of various propagation models for mobile communication," *IEEE Antennas Propag. Mag.*, vol. 45, no. 3, pp. 51–82, Jun. 2003.
[29] *LTE; Evolved Universal Terrestrial Radio Access (E-UTRA); User Equipment (UE) Radio Transmission and Reception*, document ETSI TS 36.101, ver. 14.5.0 Rel. 14, 3GPP, 2017, pp. 115–117 and 285–289.
[30] *LTE; Evolved Universal Terrestrial Radio Access (E-UTRA); Base Station (BS) Radio Transmission and Reception*, document ETSI TS 36.104, ver. 14.5.0 Rel. 14, 3GPP, 2017, pp. 50–52 and 111–113.
[31] *Technical Specification Group Services and System Aspects; Policy and Charging Control Architecture*, document TS 23.203, ver. 11.5.0 Rel. 11, 3GPP, 2012, pp. 35–38.
[32] *IMT Traffic Estimates for Years 2020 to 2030*, document M.2370-0, ITU-R, 2015, pp. 8–29.
[33] M. Chen, Y. Miao, Y. Hao, and K. Hwang, "Narrow band Internet of Things," *IEEE Access*, vol. 5, pp. 20557–20577, 2017.
[34] J. Markkula, K. Mikhaylov, and J. Haapola, "Simulating LoRaWAN: On importance of inter spreading factor interference and collision effect," in *Proc. IEEE Int. Conf. Commun. (ICC)*, May 2019, pp. 1–7.

**JUHO MARKKULA** (Student Member, IEEE) received the M.Sc. degree in telecommunications from the University of Oulu, Finland, in 2009. Since 2008, he has with the Centre for Wireless Communications, University of Oulu, where he currently works as a Research Scientist. He has worked in several research projects concerning military communications system developments. His recent works include research on smart grid communications, especially concerning LTE, wireless sensor networks, and low-power wide-area networks.

**JUSSI HAAPOLA** (Member, IEEE) received the M.Sc. degree in physical sciences and the Ph.D. degree in telecommunications engineering from the University of Oulu, Finland, in 2002 and 2010, respectively. He joined the Centre for Wireless Communications, University of Oulu, in 2001, where he currently works as a Senior Research Fellow. In 2011, he made a Postdoctoral Fellow visit with Tohoku University, Sendai, Japan. From 2012 to 2015, he was also worked with the University of Oulu Research Institute, Japan, and CWC-Nippon Ltd., as the Deputy Manager. His recent works include major contributions to two IEEE 802.15 standard amendments, and he is currently the Coordinator of the EC H2020 Project 5G!Drones under Grant 857031.